Development 138, 4969-4978 (2011) doi:10.1242/dev.070862

Targeted mutation of the *talpid3* gene in zebrafish reveals its conserved requirement for ciliogenesis and Hedgehog signalling across the vertebrates

Jin Ben[1], Stone Elworthy[2], Ashley Shu Mei Ng[1], Freek van Eeden[2] and Philip W. Ingham[1,2,3,*]

SUMMARY

Using zinc-finger nuclease-mediated mutagenesis, we have generated mutant alleles of the zebrafish orthologue of the chicken *talpid3* (*ta3*) gene, which encodes a centrosomal protein that is essential for ciliogenesis. Animals homozygous for these mutant alleles complete embryogenesis normally, but manifest a cystic kidney phenotype during the early larval stages and die within a month of hatching. Elimination of maternally derived Ta3 activity by germline replacement resulted in embryonic lethality of *ta3* homozygotes. The phenotype of such maternal and zygotic (MZ*ta3*) mutant zebrafish showed strong similarities to that of chick *ta3* mutants: absence of primary and motile cilia as well as aberrant Hedgehog (Hh) signalling, the latter manifest by the expanded domains of *engrailed* and *ptc1* expression in the somites, reduction of *nkx2.2* expression in the neural tube, symmetric pectoral fins, cyclopic eyes and an ectopic lens. GFP-tagged Gli2a localised to the basal bodies in the absence of the primary cilia and western blot analysis showed that Gli2a protein is aberrantly processed in MZ*ta3* embryos. Zygotic expression of *ta3* largely rescued the effects of maternal depletion, but the motile cilia of Kupffer's vesicle remained aberrant, resulting in laterality defects. Our findings underline the importance of the primary cilium for Hh signaling in zebrafish and reveal the conservation of Ta3 function during vertebrate evolution.

KEY WORDS: Talpid3, Zebrafish, Primary cilium, Cystic kidney, Hedgehog signalling, Gli2 processing, Ciliopathy

INTRODUCTION

Hedgehog (Hh) signalling plays a crucial role in animal development, controlling cell type specification, proliferation and survival in a variety of contexts through a pathway that has been highly conserved during evolution (reviewed by Ingham et al., 2011; Ingham and Placzek, 2006). Although originally identified through genetic analysis in *Drosophila*, many of the components that modulate and transduce Hh signals have subsequently been functionally annotated in vertebrates, both through ES cell-mediated targeted mutagenesis and via forward genetic screens in zebrafish and mouse. Unexpectedly, several of the loci identified in the latter screens were found to encode intraflagellar transport (IFT), uncovering a hitherto unsuspected role of the primary cilium in mammalian Hedgehog signalling (Eggenschwiler and Anderson, 2007) that more recent analysis of the zebrafish *oval* (that encodes the IFT88 protein) and *iguana* (*igu*) mutants has shown to be a conserved feature of Hh signalling across the vertebrates (Glazer et al., 2010; Huang and Schier, 2009; Kim et al., 2010; Tay et al., 2010). Consistent with this conservation, the chicken *talpid3* (*ta3*) mutation, originally identified on the basis of its eponymous limb defects (Ede and Kelly, 1964) and later found to disrupt transduction of Sonic hedgehog (Shh) activity in the limb as well as in the neural tube and somites (Davey et al., 2006; Lewis et al., 1999), was recently shown to identify a novel coiled-coil domain protein essential for primary ciliogenesis (Davey et al., 2006; Yin et al., 2009). Surprisingly, however, although the *ta3* gene has been highly conserved from *Nematostella* to human (Yin et al., 2009), no mutant alleles of *ta3* have been described in any other organism, despite the extensive screening efforts in mouse and zebrafish. One possible explanation for the failure to identify a zebrafish *ta3* mutant could be that maternal expression of the gene masks the effects of its zygotic inactivation. Indeed, although a number of zebrafish IFT mutants have been isolated on the basis of their ciliogenesis defects (Drummond et al., 1998; Lunt et al., 2009; Sun et al., 2004), none of these displayed the severe phenotypes seen in their mouse counterparts owing to the disruption of the Hh pathway. Only when the maternal expression of IFT88 was removed by germline replacement was the full spectrum of its effects on ciliogenesis and Hh signalling revealed (Huang and Schier, 2009).

Here, we describe the identification of the zebrafish *ta3* locus and its functional annotation via zinc-finger nuclease-mediated targeted mutagenesis. We show that maternally supplied *ta3* product is indeed sufficient to support embryogenesis in the zebrafish but that complete elimination of *ta3* function results in a phenotype strikingly similar to that of its chick counterpart. Our study provides further confirmation of the conserved role of the primary cilium in vertebrate Hh signalling and establishes a new and highly tractable model for the post-embryonic analyses of ciliopathies.

MATERIALS AND METHODS

Zebrafish strains and husbandry

Adult fish were maintained on a 14 hour light/10 hour dark cycle at 28°C in the AVA (Singapore) certificated IMCB Zebrafish Facility. Previously described zebrafish strains used were: *ptc1*^{hu1602}, *ptc2*^{tj222} (Koudijs et al., 2008); *igu*^{ts294} (Wolff et al., 2004); *Tg(eng2a:eGFP)*^{i233} (Maurya et al., 2011); and Tg(*fli::GFP*) (Lawson and Weinstein, 2002).

[1]Developmental and Biomedical Genetics Group, Institute of Molecular & Cell Biology, Proteos, 61 Biopolis Drive, Singapore 138673, Republic of Singapore. [2]MRC Centre for Developmental and Biomedical Genetics, University of Sheffield, Western Bank, Sheffield S10 2TN, UK. [3]Department of Biological Sciences, National University of Singapore, 14 Science Drive 4, Singapore 117543.

*Author for correspondence (pingham@imcb.a-star.edu.sg)

Accepted 15 September 2011

Cloning of the zebrafish *talpid3* gene

A 2220 bp 3′ expressed sequence tag (EST) clone containing the putative zebrafish *ta3* cDNA sequence (GenBank reference number XM_001338591.1) was identified by BLAST (Basic Local Alignment Search Tool) query of GenBank using the chick *Ta3* cDNA (GenBank reference number NM_001040707.1). Based on the sequence of XM_001338591.1, primers were designed for RACE experiments to identify additional 5′ and 3′ cDNA sequences. Both the 5′ and 3′ RACE experiments were performed using the SMART RACE cDNA amplification kit (BD Biosciences Clontech). The reverse primers complementary to the 5′ region of the EST sequence (5TAr1: 5′-AGTGAGAGGTGTAGACTGGGTCGG-CACT-3′) were used to amplify a 3403 bp 5′RACE. Similarly, a forward primer complementary to the 3′ region of the 5′RACE sequence (07Dec3Rf1, 5′-CAGGCTTCTCCCACACCAGTGATTCCAGC-3′) was used to amplify a 2242 bp 3′ RACE. The 4776 bp full-length cDNA (GenBank reference number JN088213) was amplified with JumpStart AccuTag LA DNA polymerase (Sigma) using the forward primer 5′-CCTGAACTACTACTGGACTAGTTACATGTTACTG-3′ (5UTRf5) and the reverse primer 5′-GCTATGAACGTCTCCAGGCACTTAGCAG-3′ (FL-07Dec3Rr2). Besides the full-length cDNA, the forward primers complementary to XM_001338591.1 EST (3TAf3, 5′-TACATCAGTGCT-GTCACATGTGCCTGCTG-3′; 2189-FP1, 5′-ACAGAGCGGCGATCCA-AACTCAGATG-3′) amplified another two different 3′RACE products, of 389 bp (GenBank reference number JN088214) and 1083 bp (GenBank reference number JN088215), respectively. The three 3′RACE products and the EST (XM_001338591.1) are non-conserved at their 3′ end, indicating the occurrence of alternative splicing.

Generation, selection and genotyping of *talpid3* mutant alleles

Zinc-finger nucleases (ZFN) specific for the zebrafish *ta3* gene were generated using Oligomerized Pool Engineering (OPEN) (Maeder et al., 2008) with selection using the bacterial one hybrid (B1H) system (Noyes et al., 2008). For the left subunit of the ZFN, OPEN pools 37 and 4 (GGCt), 108 (GGC) and 54 (GTG) were recombined by PCR and assembled in vector 1352omegaUV2 to create a phagemid library. Likewise for the right subunit; OPEN pools 3 and 41 (GGAt), 116 (TGA) and 31 (GTT) were assembled. The libraries each had ~10^7 independent clones. Bait plasmids with each required zinc-finger recognition half site sequence were constructed in a version of the pH3U3 vector modified to be chloramphenicol resistant rather than kanamycin resistant. Phage transduction was used to introduce each zinc finger protein (ZFP) library to US0 cells harbouring the respective bait plasmid and ~2×10^7 transductants were exposed to selection on 14 cm His selective (NM) plates with either 15 mM or 20 mM 3-AT. The largest looking colonies were re-streaked on NM plates with 20 mM 3-amino-1,2,4-triazole (3-AT). Sequencing of these selected clones and random clones picked prior to selection revealed that selection had induced a marked bias in the zinc-finger recognition helix residues. For each subunit, a clone with a prevalent sequence was chosen for making the ZFP. As a precaution, these chosen plasmids were retransformed into US0 cells with the respective bait plasmids to confirm growth on NM plates with 20 mM 3-AT. These selected zinc-finger domains were sub-cloned into the pCS2FlagFok1DD and pCS2HAFok1RR plasmids (Meng et al., 2008). Capped RNA from each plasmid was produced by in vitro transcription and a range of doses was injected into one-cell stage zebrafish embryos. Embryos injected with ~100 pg had an appropriate 30% rate of deformity at 24 hpf (hours post-fertilisation). Genomic DNA prepared from non-deformed 24 hpf embryos injected with this dose was used as a PCR template to analyse potential somatic mutations. The site of the ZFN target overlaps an *Nla*III endonuclease site. Amplicons from injected embryos were partially resistant to *Nla*III cleavage while the amplicons from uninjected embryos were fully cleaved. Roche Titanium 454 amplicon sequencing showed that 108 out of 693 (16%) of the amplicon molecules had insertions or deletions at the target site. G0 adults derived from embryos injected with ZFN capped RNA were in-crossed and their progenies (G1) individually genotyped by PCR using the forward primer (5′-TGGCATGTCAGC-AGAAAAACA-3′) and reverse primer (5′-TGGACTTTCTGCACTC-CCTTGC-3′) followed by Sanger sequencing.

Generation of MZ*talpid3* by germ cell replacement

Donor embryos from a $ta3^{i265}$/+ × $ta3^{i262}$/+ intercross were labelled by injecting GFPnanos3′ UTR RNA (Koprunner et al., 2001). Wild-type host embryos were injected with morpholino antisense oligonucleotide against *dead end* (5′-GCTGGGCATCCATGTCTCCGACCAT-3′) to block germ cell development (Weidinger et al., 2003). Cells were transplanted from donors (1000 cell stage) into the hosts (dome stage). Donor embryos were genotyped by PCR using the primers described above. Transplanted host embryos were screened at 24 hpf for successful transfer of donor germ cells as indicated by GFP expression (Ciruna et al., 2002).

In situ hybridization and immunofluorescence

Standard in situ hybridization was performed with anti-Dig alkaline phosphatase and chromogenic substrate NBT/BCIP as previously described (Oxtoby and Jowett, 1993). RNA probe used for in situ hybridization of *ta3* was synthesized from the 4779 full-length template and sheared into 500 bp fragments with 60 mM Na_2CO_3/40 mM $NaHCO_3$. RNA probes for other genes were prepared from templates as previously described: *ptc2* (formerly *ptc1*) (Barth and Wilson, 1995; Concordet et al., 1996), *nkx2.2* (Barth and Wilson, 1995; Concordet et al., 1996), *L-fabp* and *trypsin* (Lo et al., 2003).

Whole-mount antibody staining was performed as previously described at the following dilutions: mAb 4D9 (anti-Engrailed; DHSB) at 1:50-1:200; rabbit anti-Prox1 at 1:5000 (Elworthy et al., 2008); rabbit anti-γ-tubulin at 1:500 (Sigma); mouse anti-γ-tubulin at 1:500 (Sigma); and mouse anti-acetylated α-tubulin at 1:800 (Sigma). The secondary antibodies were: Alexa488-conjugated goat anti-mouse or anti-rabbit, Alexa546-conjugated goat anti-mouse and Alexa568-conjugated goat anti-rabbit, Alexa633-conjugated goat anti-secondary antibodies (1:1000, Invitrogen). Bright-field microscopy images were acquired with an AxioCam HRc mounted on a Zeiss AXIO Imager M2, Olympus DP70 on MVX10 or Leica DFC300 FX mounted on MZ16FA. Fluorescent specimens were imaged using the 60× or 100× oil immersion objective on an Olympus Fluoview 1000 confocal microscope. Images were acquired using Olympus FV10-ASW software.

Synthetic RNA, DNA and morpholino for injection

The full-length coding region of the zebrafish *ta3* cDNA was cloned as a *Cla*I/*Xho*I fragment immediately 3′ to the coding region of EGFP inserted into the *Bam*HI/*Cla*I sites in the polylinker of pCS2+ (Turner and Weintraub, 1994) to generate a C-terminal in-frame fusion with EGFP. The plasmid was linearized with *Sac*II. pCS2-GFP-Kif7 (Tay et al., 2005) and pCS2-GFP-Dzip1 (Kim et al., 2010) were linearized with *Not*I. Capped synthetic mRNAs were transcribed in vitro with SP6 mMessage mMachine Kit (Ambion) and injected into fertilized eggs. BAC Gli2a-GFP was used as previously reported (Kim et al., 2010).

Cyclopamine treatment of embryos

Cyclopamine treatment followed a standard method with immersion in 40 μM cyclopamine (Toronto Research Chemicals) from the bud stage as previously described (Wolff et al., 2003).

Western blot analysis

Embryos were dechorionated, deyolked and homogenized manually in ice-cold PBS without Ca^{2+} and Mg^{2+} in the presence of complete protease inhibitor cocktail (Roche). The embryo pellet was lysed in RIPA buffer [50 mM Tris HCl (pH 8.0), 150 mM NaCl, 1% NP-40, 0.5% sodium deoxycholate, 0.1% SDS, protease inhibitor cocktail and 1 mM PMSF]. Samples were microcentrifuged for 10 minutes at 4°C, loading buffer [62.6 mM Tris HCl (pH 6.8), 2% SDS, 0.01% bromophenol blue, 10% glycerol and 100 mM DTT] was added to the supernatant and the equivalent of 30 embryos run on each lane of a 7.5% acrylamide denaturing gel at 30 mA for 120 minutes, and electroblotted onto Immobilon-P polyvinylidene fluoride (PVDF) membrane (Millipore). PVDF strips were blocked in 5% milk powder PBS 0.1% Tween20 for 1 hour, and incubated with rabbit anti-zebrafish Gli2a (1:5000) (Maurya et al., 2011) for 1 hour at room temperature. After washing, primary antibody was detected with ECL HRP-conjugated anti-rabbit IgG (1:50,000). Chemiluminescent Substrate was SuperSignal

West Femto (Pierce). The loading amount of protein extract among specimens was evaluated by β-actin level with rabbit anti-β-actin (1:5000; Cell Signalling). Signal quantification was performed using Adobe Photoshop software.

RESULTS

Conserved synteny and sequence similarity identifies the zebrafish *talpid3* orthologue

We amplified a 4.7 kb full-length cDNA (see Materials and methods) predicted to encode a 1554 amino acid protein (supplementary material Fig. S1) with 33/50%, 31/45%, 33/49% and 35/51% sequence identity/similarity to the chicken, human, mouse and *Xenopus* Ta3 proteins, respectively. The coding sequence of the zebrafish *ta3* gene consists of 31 exons, conceptual translation of which predicts an encoded protein with five coiled-coiled motifs (Fig. 1B; supplementary material Fig. S2). The genomic sequence is located on linkage group 17 (LG17) in a syntenic region conserved between zebrafish, *Xenopus*, chick, mouse and human (Fig. 1A).

Ubiquitously distributed zebrafish *talpid3* mRNA encodes a protein that localizes to the basal body and centriole

In situ hybridization revealed that newly fertilized eggs contain abundant maternally derived *ta3* mRNA. The *ta3* transcript is ubiquitously distributed in embryos from early cleavage stages through to 2 dpf (Fig. 1C,D). To investigate the subcellular distribution of the Ta3 protein in zebrafish embryos, we generated a construct encoding the Ta3 protein fused at its N terminus to EGFP (see Materials and methods) and injected mRNA transcribed from this construct into newly fertilized eggs. The EGFP-Ta3 fusion protein localized to the basal body and to its daughter centriole in somitic cells of wild-type embryos (Fig. 1E). Localization to the basal body was unaffected by the loss of wild-type Dzip1 protein in *iguana* mutants (Fig. 1F).

Generation of mutant alleles of zebrafish *talpid3* using zinc-finger nucleases

To analyse the function of *talpid3* in the zebrafish embryo, we initially used the well-established approach of morpholino oligonucelotide mediated gene knockdown (Eisen and Smith, 2008). Morpholinos designed to block either translation or splicing of the *ta3* transcript (supplementary material Fig. S3) were injected into newly fertilized embryos following standard protocols and the injected embryos were fixed and assayed for expression of Prox1 and Engrailed proteins, two sensitive read-outs of Hh pathway activity in the zebrafish myotome (Wolff et al., 2003), and for acetylated α-tubulin, a marker for cilia. Using three different morpholinos at varying concentrations, we failed to observe any reproducible changes in Prox1 or Eng expression or any cilium defects (data not shown).

Accordingly, we adopted a different strategy to inactivate *ta3* function, namely the generation of stable germ line transmissible mutant alleles using zinc-finger nuclease (ZFN)-mediated targeted mutagenesis (Doyon et al., 2008; Foley et al., 2009; Meng et al., 2008). The online ZiFiT software was used to identify sequences in the *ta3*-coding region that are potentially amenable to targeted mutagenesis using the OPEN ZFN method (Maeder et al., 2008). Targeting this sequence (aGCCGCCCACgtccatGTTTGAGGAt) in the eleventh coding exon had the potential to create mutations at Thr 553 (Fig. 2A) in a region conserved with the chick Ta3 protein. This site was chosen in preference to others (including some closer to the N terminus) based on the notion that OPEN zinc-finger nucleases with first and third fingers directed against GNN recognition sites and middle fingers directed against either G/TNN recognition sites

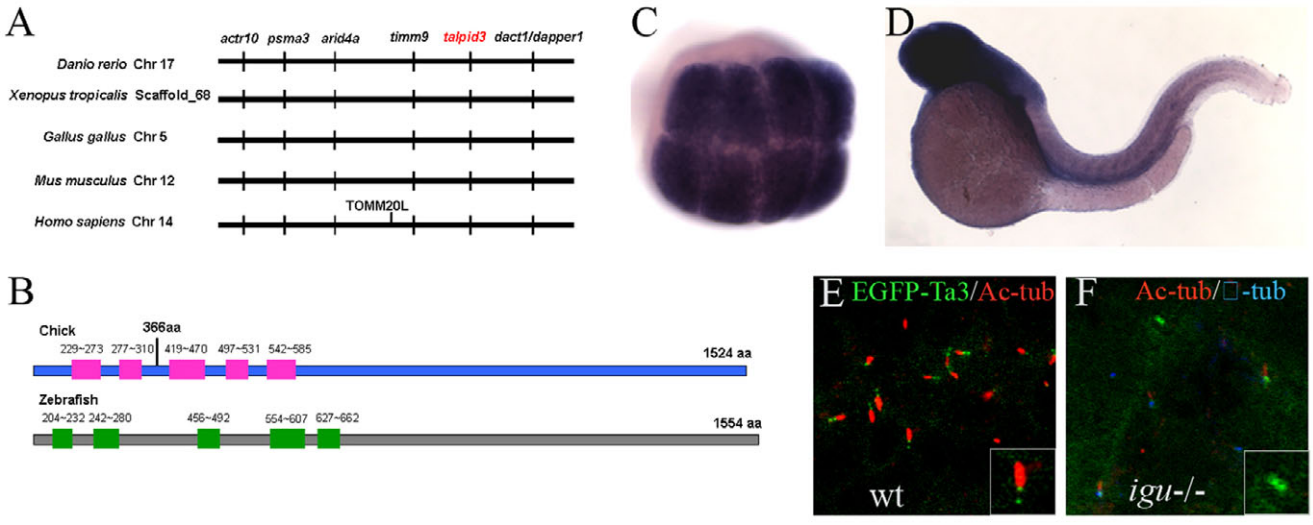

Fig. 1. Genomic location, expression, domain structure and subcellular localization of *talpid3* and its encoded protein. (**A**) The chicken (*Gallus gallus*) *ta3* locus is located in a region of chromosome 5 that shows conserved synteny with zebrafish (*Danio rerio*) chromosome 17, mouse (*Mus musculus*) chromosome 12 and human (*Homo sapiens*) chromosome 14 (based on UCSC genome browser). (**B**) Schematic representation of the chicken and zebrafish Talpid proteins showing the five coiled-coil domains in each (pink and green boxes, respectively) predicted using the program in http://groups.csail.mit.edu/cb/multicoil/cgi-bin/multicoil.cgi/cgi-bin/multicoil. Despite the low sequence identity (33%) between the two proteins, the number and distribution of coiled-coil domains are conserved. The location of the lesion associated with the chick *ta3* mutant allele at residue 366 between the 1st and 2nd coiled-coil domains is indicated. (**C**,**D**) Distribution of *ta3* mRNA revealed by in situ hybridization of early cleavage stage (C) or 2 dpf (D) embryos. Note the abundant maternally derived transcript in C. (**E**,**F**) GFP-tagged Talpid3 protein localizes to the basal body and the daughter centriole in cells of wild-type embryos (E). This localization is unaffected by mutation of *igu*, which encodes the basal body protein Dzip1 (F).

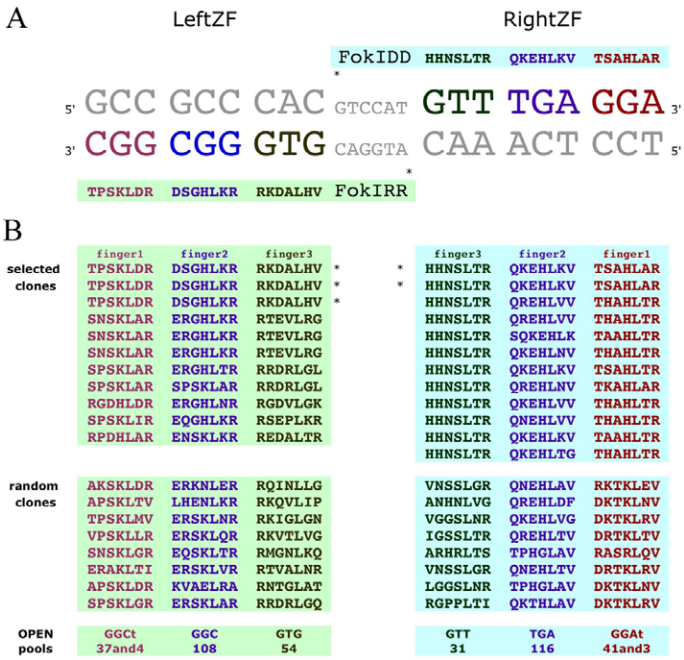

Fig. 2. Targeted mutagenesis of the zebrafish *ta3* locus. (**A**) Nucleotide sequence of the zebrafish *ta3* gene chosen for targeting and amino acid sequences of the zinc-finger proteins selected to recognize this sequence. Each of the latter was fused to a subunit of the FokI nuclease as shown. (**B**) Sequences of zinc-finger clones selected (upper block) or picked at random (lower block) from the OPEN pools for each triplet motif (bottom row). Asterisks indicate the sequences chosen for use as the mutagenic left and right zinc-finger proteins (ZFP) as shown in A.

might be more effective (Ramirez et al., 2008). Embryos injected with mRNA encoding a ZFN pair selected for recognition of this sequence were found to carry a variety of deletions or insertions at the target site (data not shown) confirming the efficacy of this approach. Accordingly, we grew up adults from injected embryos and screened their progeny for similar lesions in *ta3*. In this way, we recovered a number of individuals transmitting insertion or deletion mutations, several of which cause frameshifts resulting in premature termination codons (Table 1) predicted to yield proteins truncated N terminal to the fourth coiled-coil domain.

Loss of zygotic *talpid3* function causes a cystic kidney phenotype

Animals trans-heterozygous for *ta3* mutant alleles predicted to encode truncated proteins completed embryogenesis and showed no defects in Eng or Prox1 expression in the myotome, nor any other manifestations of aberrant Hh pathway activity (data not shown). Consistent with this, the growth and morphology of the primary cilia appeared normal. By 4 dpf, however, some mutant larvae displayed dilation of the pronephric tubules and edema (Fig. 3B). Confocal analysis revealed that cilia became sparsely distributed within the pronephric tubules, which displayed an apparent overproliferation of epithelial cells (Fig. 3D). There was no evidence of body curvature typical of other zebrafish cilia mutants (Drummond et al., 1998; Lunt et al., 2009; Pathak et al., 2007; Sun et al., 2004). Most *ta3* trans heterozygotes died before 14 dpf, although some could survive for up to 4-5 weeks. By contrast, animals homozygous for the $ta3^{i267}$ allele, which causes a small 81 nucleotide in-frame deletion, were almost fully adult viable (Fig. 3E).

Loss of maternally derived *talpid3* activity disrupts Hh signalling

We surmised that the lack of a mutant phenotype in trans heterozygous *ta3* embryos could be due to the significant levels of maternally derived *ta3* mRNA present in newly fertilized eggs. To test this inference, we used the germ cell replacement technique (Ciruna et al., 2002) to generate chimeric females with *ta3* mutant germ lines (see Materials and methods for details) and crossed these to $ta3^{i264}$/+ heterozygous males. The resulting MZ (maternal + zygotic) *ta3* mutant embryos exhibited a curled body and ectopic lens phenotype at 1 dpf (Fig. 4A,C). The domain of Eng expression was significantly expanded among the fast muscle fibres by 28 hpf, indicative of an increased number of Hedgehog-dependent MFFs (Fig. 4E,G). At the same stage, transcription of *ptc2* was upregulated in the somites but downregulated in the neural tube, whereas expression of *nkx2.2* was almost eliminated from the ventral neural tube (Fig. 4I,M). Treatment with the Smo antagonist cyclopamine had no effect on *ptc2* or *nkx2.2* expression in MZ*ta3* embryos (Fig. 4K and data not shown), indicating that transduction of the Hh signal is disrupted downstream of Smo. By 2 dpf, the embryos exhibited mild cyclopia (Fig. 5A,B). Expression of the *fli::GFP reporter* revealed mis-branching and merging of the cerebellar central artery, which is associated with hindbrain haemorrhage, in over 70% of embryos (Fig. 5F,G). The pectoral fins of 4 dpf larvae were symmetric (Fig. 5D), reminiscent of the polydactylous limbs typical of the chick *ta3* mutant. This phenotypic spectrum is very similar to that of *iguana* homozygotes (Sekimizu et al., 2004; Wolff et al., 2004) and of MZ*ift88* mutant embryos (Huang and Schier, 2009). The MZ*ta3* mutants died at 4 dpf. By contrast, *ta3*/+ heterozygotes derived from *ta3* homozygous mutant oocytes (designated M*ta3*) showed no evidence of aberrant Hh pathway activity, their patterns of Hh-target gene expression being indistinguishable from wild-type embryos.

Loss of maternally derived *talpid3* activity disrupts ciliogenesis

Confocal analysis of MZ*ta3* embryos stained with anti-acetylated tubulin revealed a complete absence of both motile and primary cilia (Fig. 6, Fig. 7D). The loss of primary cilia is consistent with the evidence of aberrant Hh pathway activity in MZ*ta3* embryos described in the preceding section. In wild-type embryos, GFP-tagged Gli2a has been shown to accumulate at the tip of primary cilia in response to Hh pathway activation, whereas similarly tagged DZIP1 protein encoded by *igu* accumulated at the basal body (Kim et al., 2010) (Fig. 6G,M). Using the same GFP fusion constructs, we investigated the localization of both proteins in the absence of primary cilia in MZ*ta3* mutants. The basal body localization of DZIP1-GFP was unchanged (Fig. 6J), whereas Gli2a-GFP now also localized to the basal body (Fig. 6H). Similarly, GFP-Kif7, which, in wild-type embryos, was enriched along the axoneme or at the tip of primary cilium (Fig. 6K), also accumulated at the basal body in the absence of the cilium in MZ*ta3* mutants (Fig. 6L).

In zygotically rescued M*ta3* embryos, primary cilia and motile cilia in the pronephric duct developed relatively normally; however, the number and length of motile cilia present in Kupffer's vesicle varied significantly compared with wild type (Fig. 7B,C). To assess the effects of these abnormalities, we examined laterality by the orientation of two asymmetrically located endodermal organs, the liver and exocrine pancreas (Chen et al., 2001), using

Table 1. Alleles and translational products of zebrafish *talpid3* mutants generated with OPEN-ZFN

Alleles	Genotypes and encoded Talpid3 proteins
Wild type	AGAGCATCCAGCCGCCCACGTCCATGTTTGAGGATGCAGGACTGG S I Q P P T_{552} S M F E D A G L
ta3^{i262} (18to5 bp)	AGAGCACGTTCTGTTTGAGGATGCAGGACTGGTCC**TGA**GGCAGGTCA S_{547} T F C L R M Q D W S *
ta3^{i263} (CCATins)	AGAGCATCCAGCCGCCCACGTCCATCCATGTTT**TGA**GGATGCAGGACTGG S I Q P P T S_{553} I H V *
ta3^{i264} (17bpins)	AGAGCATCCAGCCGCCCACGTCCATGGGGCTTGAGGAAGCAGGTTTGAGGATGCAGGACTGGTCC**TGA** S I Q P P T S M_{554} G L E E A G L R M Q D W S *
ta3^{i265} (Cins)	AGAGCATCCAGCCGCCCACGCTCCATGTTT**TGA**GGATGCAGGACTGG S I Q P P T_{552} L H V *
ta3^{i266} (CCACGdel)	AGAGCATCCAGCCGC*TC*CATGTTT**TGA**GGATGCAGGACTGGTCCTGAGG S I Q P_{553} L H V *
ta3^{i267} (81bp-del)	CCCTCCATGTTTGAGGATGCAGGACTG P S M F E D A G L
ta3^{i268} (6bp-del)	AGAGCATCCAGCCGCCCACGTTTGAGGATGCAGGACTGG S I Q P P T_{552} F E D A G L

in situ hybridization for *l-fabp* and *trypsin* respectively. Compared with wild type in which just 2.7% of larvae showed laterality reversal, such reversals were observed in 24.7% of M*ta3* embryos. Among MZ*ta3* embryos, the endodermal organs were absent in 51.7% of individuals, but when present showed randomized orientation (Fig. 7E-J). The absence of endodermal organs is consistent with a disruption of Hh pathway activity.

Aberrant Gli2a processing in the absence of primary cilia

Several lines of evidence have implicated the primary cilium as the processing hub for Gli proteins. To explore this role further, we analysed Gli2a processing by western blot analysis of protein extracts from wild-type and MZ*ta3* mutant embryos at 28 hpf. We used a polyclonal antibody raised against a region N-terminal to the cleavage site of the zebrafish Gli2a protein (Maurya et al., 2011), which therefore can detect both the full-length (activator) form (Gli2aFL) and the truncated repressor form (Gli2aR). Extracts from wild-type embryos showed two prominent bands when probed with this antibody, one of around 190 kDa, corresponding to Gli2aFL, and one of around 48 kDa, corresponding to Gli2aR (Fig. 8, lane 3). The levels of the larger band were significantly diminished whereas those of the smaller band were significantly increased in embryos treated with cyclopamine (Fig. 8, lane 1) such that the FL:R ratio was reduced from 0.45 typical of wild type to 0.05. Conversely, the presumed Gli2aR band was significantly diminished, whereas the intensity of the Gli2aFL band increased slightly in *ptc1*^{hu1602}*; ptc2*^{tj222} double mutant embryos (Fig. 8, lane 2) the FL:R ratio increasing fourfold relative to wild type. These findings are consistent with a major role for HH in the modulation of Gli2a processing. In MZ*ta3* extracts, the level of Gli2aR was slightly reduced compared with that of wild-type extracts, whereas the level of the Gl2aFL form was slightly enhanced (Fig. 8, lane 4), such that the FL:R ratio increased to 0.6; in addition, multiple forms of intermediate size could now be detected. In contrast to wild-type embryos, cyclopamine treatment

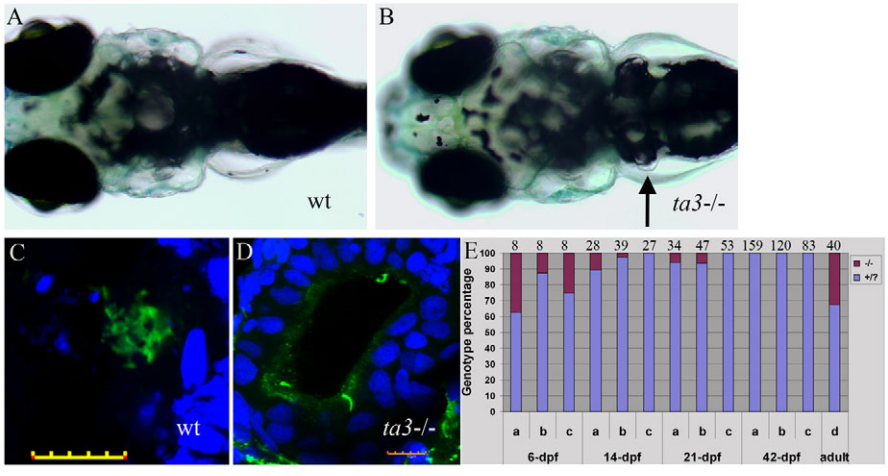

Fig. 3. Zygotic loss of *ta3* causes cystic kidney phenotype and larval lethality. (**A**,**B**) Wild-type (A) and *ta3*^{i265}/*ta3*^{i262} trans-heterozygous mutant (B) larvae at 8 dpf showing the characteristic nephron 'bubble' (arrow in B). (**C**,**D**) Optical sections of pronephric tubules from wild-type (C) and *ta3*^{i265}/*ta3*^{i262} mutant (D) larvae stained with anti-acetylated tubulin (green) to mark the axonemes of cilia and DAPI (blue) to mark nuclei; note the increased number of nuclei and the reduced number of cilia (green) in the dilated tubule lumen of the mutant compared with the narrow lumen and densely packed cilia in wild type. Scale bars: 10 μm. (**E**) Histogram showing percentage of animals transheterozygous for three different allelic combinations: (a) *ta3*^{i262}× *ta3*^{i264}*;* (b) *ta3*^{i268}/*ta3*^{i266}× *ta3*^{i263}*;* (c) *ta3*^{i265}× *ta3*^{i262} (represented by red shading) relative to heterozygous and homozygous wild-type siblings (represented by blue shading) 6, 14, 21 and 42 days post-fertilization (dpf). Most trans-heteroygotes fail to survive beyond 42 dpf. Animals homozygous for *ta3*^{i267} (d) are almost fully adult viable. The numbers above each column indicate the sample size.

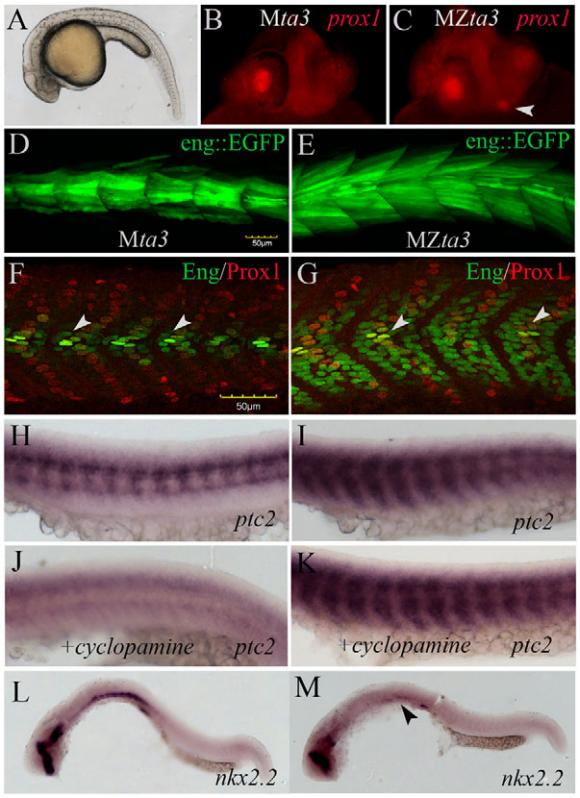

Fig. 4. Disrupted Hh signalling in the somites and neural tube of Zebrafish MZ*ta3* mutant embryos. (**A-C**) MZ*ta3* mutant 24 hpf embryos display a characteristic curled body (A) and ectopic lens marked by the expression of Prox1 (arrowhead) (C). (**D**,**E**). Expanded domain of *eng2a:GFP* reporter gene expression in MZ*ta3* (E) relative to control, zygotically rescued M*ta3* heterozygotes (D). (**F**,**G**) Antibody staining of endogenous Eng and Prox1 proteins reveals that expansion of Eng is specific to the Prox1-negative fast-twitch muscle fibres; conversely, there is a reduction in the number of Eng expressing slow-twitch muscle pioneer fibres (arrowheads). (**H**,**I**) Expression of *ptc2* in somites of M*ta3* (H) and MZ*ta3* (I) embryos showing expansion in latter. (**J**,**K**) Expression of *ptc2* in somites of M*ta3* (J) and MZ*ta3* (K) embryos following incubation in cyclopamine. (**L**,**M**) Expression of *nkx2.2* in the ventral neural tube (L) is lost in MZ*ta3* mutants (M, arrowhead).

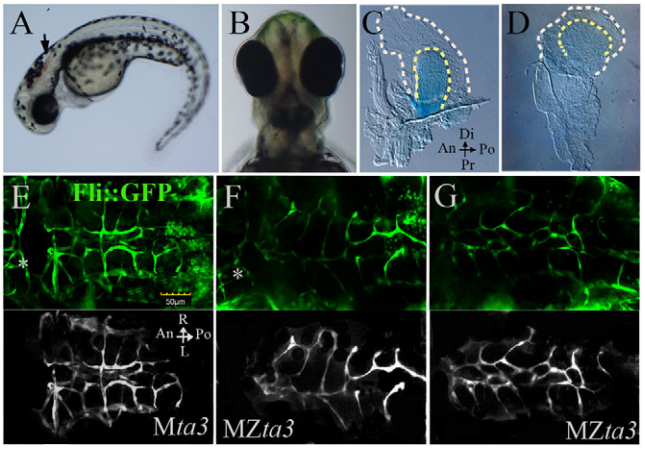

Fig. 5. Fin and head abnormalities in MZ*ta3* mutants. (**A**,**B**) MZ*ta3* embryos at 2 dpf displaying hindbrain haemorrhage (arrow) and mild cyclopia (B). (**C**,**D**) Pectoral fins from M*ta3* and MZ*ta3* larvae stained with Alcian Blue, showing loss of asymmetry in mutant (D). Broken lines indicate the fin fold margin. (**E-G**) Cranial blood vessels marked by the fli::GFP transgene; background had been removed in lower monochrome panels for ease of observation. Note the mis-branched and merged vessels of the cerebellar central artery in the MZta3 embryos (F,G), beneath the haemorrhagic area. Posterior mesencephalic central artery is indicated by an asterisk. An, anterior; Po, posterior; Di, distal; Pr, proximal; L, left; R, right.

of MZ*ta3* embryos caused only a slight reduction in the FL:R ratio (Fig. 8, lane 6); interestingly, the FL:R in M*ta3* embryos was also only slightly reduced after cyclopamine treatment (Fig. 8, lane 7).

DISCUSSION

Based on sequence comparison and synteny analysis, we have identified the zebrafish orthologue of the chicken *ta3* gene, previously shown to encode a centrosomal protein that is essential for primary ciliogenesis (Yin et al., 2009). Consistent with these properties, we found that a zebrafish EGFP-Ta3 fusion protein localizes both to the basal body and to the daughter centriole in zebrafish embryonic cells. Our initial attempts to analyse *ta3* function in the zebrafish using morpholino antisense oligonucleotides proved unsuccessful, highlighting the limitations of this approach (Eisen and Smith, 2008). To circumvent this problem, we used a previously described targeted mutagenesis approach (Doyon et al., 2008; Foley et al., 2009; Meng et al., 2008) to generate stable germline transmissible alleles of the zebrafish *ta3* gene. Zinc-finger nucleases that recognise sequences close to the 5′ end of the gene were selected using the OPEN protocol. These reagents proved highly mutagenic when injected into zebrafish embryos, generating deletion and insertion mutations at high frequency. In contrast to their chicken counterpart, however, these zebrafish *ta3* mutations proved to be embryonic viable, perhaps explaining why the *ta3* locus had not previously been identified in the large-scale forward genetic screens performed in this species (Haffter and Nusslein-Volhard, 1996). By contrast, elimination of both zygotic and maternal *ta3* activity achieved by germline replacement, resulted in a complex phenotype very similar to that of the chicken *ta3* mutant, (Ede et al., 1974; Ede and Kelly, 1964; Head et al., 1992; Hinchliffe and Thorogood, 1974; Lee and Ede, 1989; Lewis et al., 1999), including defects in the neural tube, somites, limbs and craniofacial structures. In the neural tube, the loss of expression of the ventral marker *nkx2.2* precisely mirrors the chick mutant phenotype and is indicative of a loss of Hh activity, as is the absence of liver and pancreas (Roy et al., 2001), that was seen in a significant proportion of mutant embryos; conversely, in the myotome, expansion of the Eng expression domain is consistent with a gain of Hh signalling (Wolff et al., 2003) and in line with this, we also found a significant expansion of the *ptc2* expression domain in the somites. This latter effect mirrors the expansion of *ptc2* expression throughout the somites of chick *ta3* embryos, although we note that these mutants also exhibit a significant downregulation of *ptc2* in the medial somite (Davey et al., 2006), an effect indicative of a reduction in Hh pathway activity.

The MZ*ta3* phenotype is strikingly similar to that of mutant alleles of the *iguana* (*igu*) gene, the product of which, DZIP1, is another coiled-coil domain protein (Sekimizu et al., 2004; Wolff et al., 2004) also required for primary ciliogenesis (Glazer et al., 2010; Kim et al., 2010; Tay et al., 2010). In contrast to Ta3, DZIP1 protein localizes uniquely to the basal body and not to the daughter centriole (Kim et al., 2010; Tay et al., 2010); we found

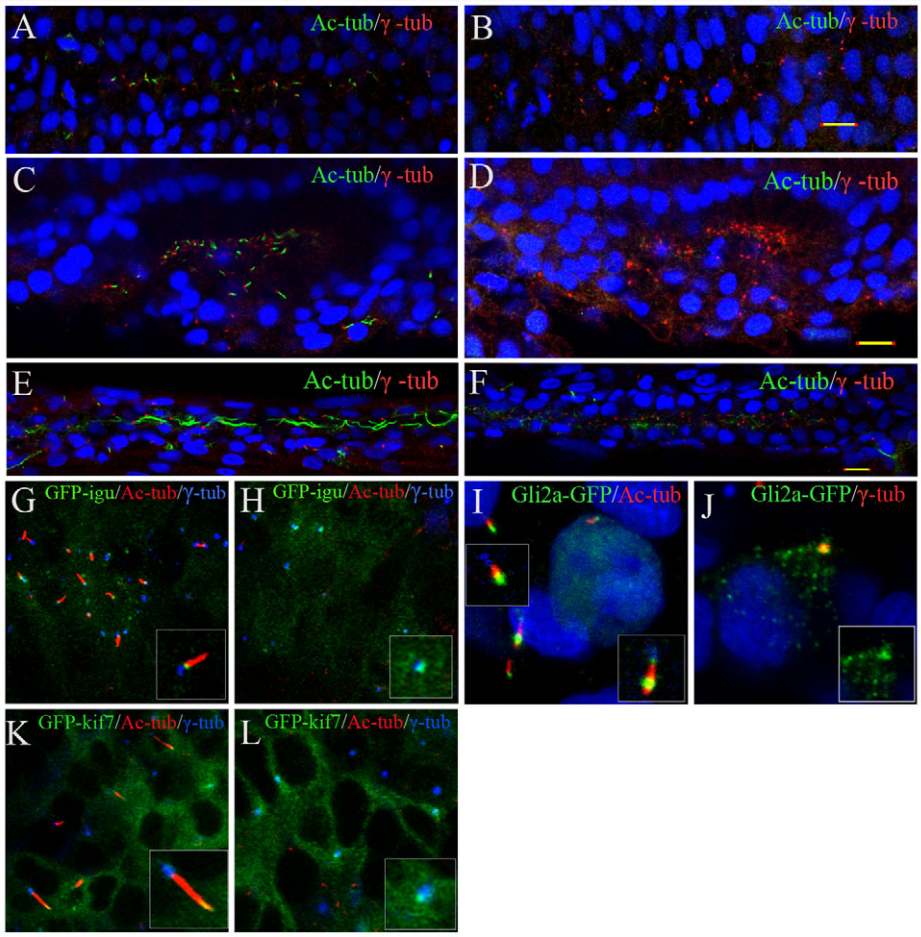

Fig. 6. Disruption of primary ciliogenesis and aberrant localization of Hh signalling components in MZ*ta3* embryos. (**A-D**) Confocal images of embryos fixed at the 10-somite (A,B) or 14-somite stage (C,D), and double stained with anti-acetylated tubulin (green) and anti-γ tubulin (red) revealing the absence of cilia from the neural tube (B) and otic vesicle (D) of MZ*ta3* mutants. (**E**,**F**) Similar preparations of embryos fixed at 24 hpf showing absence of long motile cilia from the pronephric duct of MZ*ta3* mutants (F). (**G-L**) Localization of Hh pathway components in the primary cilia of somitic cells in 5- to 10-somite stage wild-type and MZ*ta3* mutant embryos. Accumulation of a GFP-Dzip1 fusion protein in the basal body (G) is unaffected in MZ*ta3* embryos (H). (I,K) GFP-tagged forms of Gli2a (I) and Kif7 (K) accumulate at the tip of primary cilia in wild-type cells; in the absence of the primary cilium in MZ*ta3* embryos, both proteins shows a punctate localization in the basal body (J,L).

this localization to be unaffected in MZ*ta3* mutant embryos, arguing against a direct interaction between the two proteins. Likewise, and less surprisingly, the basal body localization of Ta3 appears independent of DZIP1. Although our analysis has focused on the effects of elimination of maternally derived *ta3* gene function on embryonic development, we note that it also demonstrates that *ta3* activity in the germ line is dispensable for oogenesis. We also generated males carrying *ta3* mutant germ lines; although these displayed reduced fertility, they were able to give rise to viable progeny at low frequency, in contrast to the reported sterility of chimeric *ovl*$^{tz288b/tz288b}$ (*ift88*) males (Huang and Schier, 2009).

The response of cells to Hh signalling is mediated by the Gli2 and Gli3 proteins, both of which are characterized by an N-terminal repressor domain and a C-terminal activator domain, giving them the potential to act as bi-functional transcription factors. Various lines of evidence suggest that in mammals, Gli2 acts principally as an activator (Bai and Joyner, 2001), whereas Gli3 functions both as a repressor and activator (Wang et al., 2000; Motoyama et al., 2003). In line with this, Hh abrogates the efficient processing of Gli3 to its truncated repressor form that occurs in unstimulated cells (Litingtung et al., 2002; Wang et al., 2000), while Gli2 protein is only inefficiently processed even in the absence of Hh activity (Pan et al., 2006). Previous studies of chicken *ta3* function investigated the processing of Gli3 in mutant embryos and found it to be significantly abrogated, resulting in a marked increase in the levels of the full-length form of the protein relative to its truncated repressor form (Davey et al., 2006). These findings are consistent with the Hh gain-of-function aspects of the *ta3* mutant phenotype, though are less easy to reconcile with the loss of Hh-dependent gene expression seen in the neural tube.

Zebrafish have a single Gli3 protein but two Gli2 proteins, designated Gli2a and Gli2b, the former appearing to be the orthologue of mammalian and avian Gli2 based on sequence comparisons and conserved synteny (Karlstrom et al., 1999). Notably, the expression of Gli2b and Gli3 appears largely confined to the neurectoderm and its derivatives (Tyurina et al., 2005; Ke et al., 2008), whereas Gli2a is expressed more widely in mesodermal and ectodermal derivatives (Karlstrom et al., 2003). Moreover, functional analyses suggest that, in zebrafish, both Gli3 and Gli2 act as repressors and activators; although no reagents are available to study zebrafish Gli3 protein processing, we found a significant proportion of the Gli2a protein to be in the truncated 'repressor' form, a proportion that was markedly increased upon treatment of embryos with the Smo inhibitor cyclopamine and markedly decreased in the absence of Ptc activity. These findings suggest that, in zebrafish, modulation of Gli2a processing is an important mode of control of its activity by Hh signalling. In this context it is interesting that the so-called processing determinant domain (PDD) of Gli2 identified by Pan and Wang (Pan and Wang, 2007) shows 84% sequence identity between mouse and human but only 52% identity between zebrafish and mouse (supplementary material Fig. S4). Whether or not this divergence in sequence is sufficient to confer the differing Gli2 processing profiles observed between mouse and fish remains to be determined.

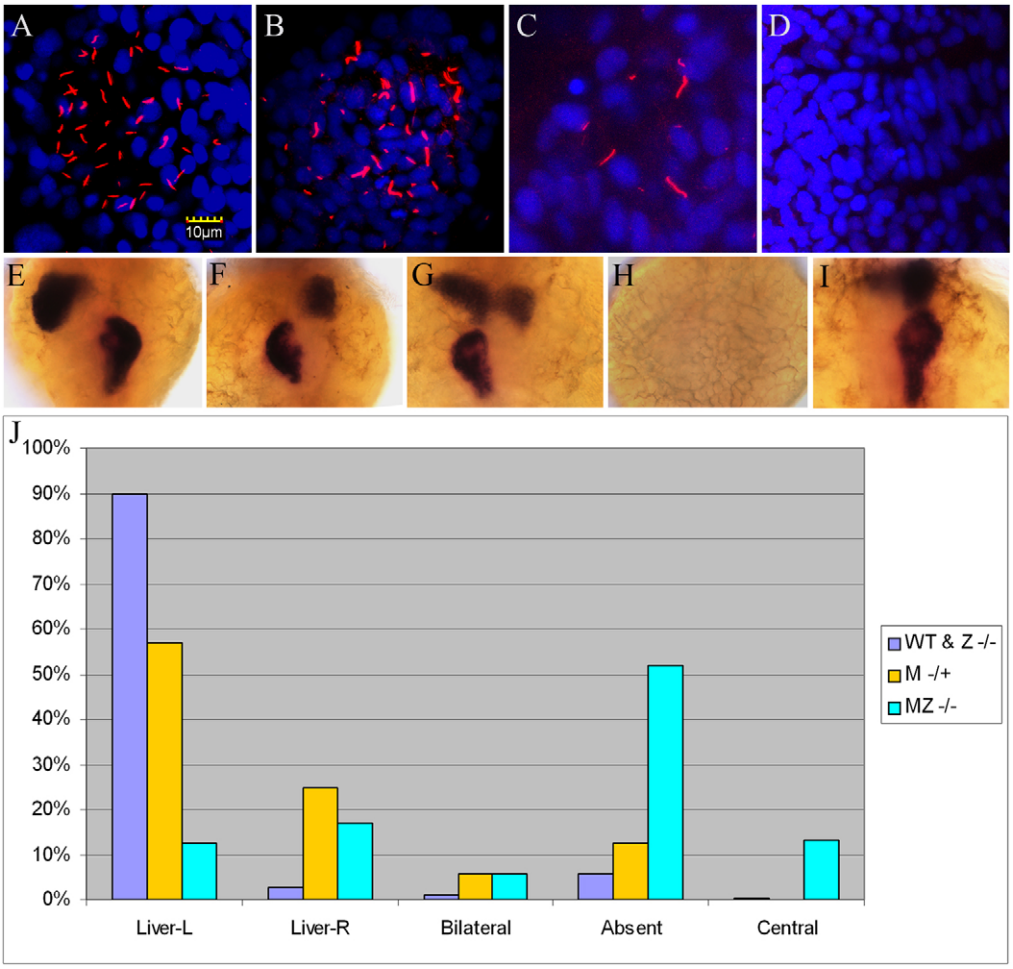

Fig. 7. Disruption of left-right asymmetry in M*ta3* and MZ*ta3* mutants. (**A-D**) Confocal images of embryos stained with anti-acetylated tubulin (red) and DAPI (blue) showing Kupffer's vesicle in wild-type (A) M*ta3* (B,C) and MZta3 (D). Note the variable number and length of motile cilia in M*ta3* embryos compared with wild type. (**E-I**) Examples of liver and exocrine pancreas orientation revealed by in situ hybridization for the liver marker *l-fabp* and the pancreas marker *trypsin*. Orientations are categorized into five phenotypes: left liver and right pancreas, typical of wild-type (E), right liver and left pancreas (F), bilateral (G), absent (H), and centralized liver and pancreas (I). (**J**) Frequency distribution of different phenotypes among wild-type and *ta3/ta3* embryos, and M*ta3* and MZ*ta3* mutant embryos.

In contrast to the major abrogation of Gli3 processing seen in chick *ta3* mutants (Davey et al., 2006), we found the reduction in Gli2aR levels in zebrafish MZ*ta3* to be less dramatic. At the same time, we observed a slight increase in the levels of full-length Gli2a, as well as the appearance of bands of intermediate size, that are not detected at significant levels in wild-type embryos or in the absence of Smo or Ptc activity. One limitation of our analysis is that it was performed on whole-embryos extracts, making it impossible to relate the changes in Gli2a species to the contrasting effects on Hh target gene expression in different tissues. Moreover, in order to identify mutant embryos unequivocally on the basis of their phenotype, we were limited to analyzing Gli2a at 28 hpf, which is several hours after the crucial period for muscle cell type specification (Wolff et al., 2003). Nevertheless, the modest increase in Gli2a FL;R ratio is consistent with the apparent gain-of-function Hh phenotypes observed in MZ*ta3* mutants. The fact that the pattern of processing was largely unaltered in response to cyclopamine treatment is in line with the failure of cyclopamine to modify the MZ*ta3* phenotype and underlines the importance of the primary cilium as a hub for the modulation of Gli processing by Hh. Interestingly, we found that a GFP-tagged form of Gli2a that normally shuttles to the tip of the primary cilium in response to Hh activity (Kim et al., 2010) localizes to the basal body in MZ*ta3* mutants. Similarly, we found that GFP-tagged Kif7 also localizes to the basal body in the absence of the primary cilium, consistent with the notion that Kif7 sequesters Gli proteins at the basal body

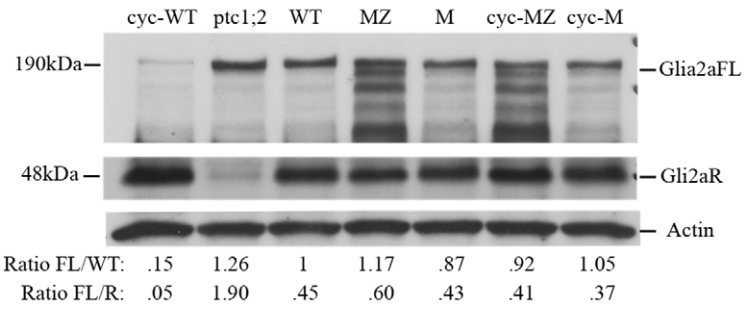

Fig. 8. Processing of Gli2a is regulated by Hh activity and is disrupted in *ta3* mutant embryos. Western blot of extracts of 28 hpf embryos probed with anti-Gli2a antibody. The full-length Gli2aFL form runs with apparent molecular weight of ~190 kDa and the truncated Gli2aR form with an apparent molecular weight of ~48 kDa. The same filter was probed with anti-actin, which serves as a loading control. Numbers below each lane show the level of Gli2aFL relative to that in wild-type normalized to control and the FL:R ratio for each sample based on densitometric analysis of filters exposed for identical times. Note, however, that the three panels shown here were exposed for different lengths of times for the purpose of clarity of presentation. Cyc, cyclopamine treated; M, M*ta3* embryos; MZ, MZ*ta3* embryos.

in the absence of Hh activity. We note, however, that the FL form of Gli2a also appeared resistant to cyclopamine treatment in M*ta3* embryos, despite their having normal primary cilia and showing sensitivity to cyclopamine treatment at the level of Hh gene expression.

Disruption of left-right (LR) asymmetry is one aspect of the zebrafish MZta3 phenotype that is not shared with the chick mutant (Davey et al., 2006), though a similar effect has recently been described in mouse *ta3* homozygotes (Bangs et al., 2011). Previous studies have shown that ectopic Shh activity can cause reversals of L-R patterning, as indicated by changes in laterality of the heart and endodermal organs (Levin et al., 1995; Schilling et al., 1999). Thus, the effects seen in MZ*ta3* embryos could reflect the partial de-repression of Hh pathway activity due to the loss of primary cilia. Significantly, however, we observed LR abnormalities in zygotically rescued embryos derived from *ta3* mutant oocytes (M*ta3*) in which there is no evidence of aberrant Hh pathway activity but there is depletion of the motile cilia in Kupffer's vesicle. Given the implication of nodal flow in establishing LR asymmetry (Hirokawa et al., 2006), we consider it most likely to be the disruption of motile ciliogenesis that underlies this particular aspect of the *ta3* phenotype. With the exception of this requirement, which probably reflects the precocious differentiation of motile cilia in Kupffer's vesicle, maternally derived *ta3* product appears dispensable for normal development; at the same time, the zygotic *ta3* phenotype indicates that maternally derived Ta3 is sufficient to support embryogenesis, as *ta3* homozygotes first manifest a mutant phenotype, cystic kidneys, only during early larval stages. A similar phenotype has also been reported to develop in chick *ta3* mutants at 7 days (Yin et al., 2009) and has also been described in a number of different zebrafish mutants, most of which have been found to disrupt genes encoding either centrosomal or IFT proteins (Drummond et al., 1998; Lunt et al., 2009; Pathak et al., 2007; Sun et al., 2004). In contrast to *ta3*, however, these zebrafish cystic kidney mutants have other phenotypic effects that manifest in the embryo leading to early lethality. In this respect, the late larval lethality of the *ta3* mutant makes it an especially useful model for PKD and potentially for other ciliopathies.

Acknowledgements
We thank Iain Drummond for helpful suggestions, Sudipto Roy for the *Kif7-GFP* construct, Ashish Maurya for providing the *eng2a:GFP* reporter line, Cheryll Tickle for communicating data ahead of publication, and colleagues at ICMB and the MRC CDBG for their interest and advice.

Funding
This research was supported by the Singapore Biomedical Research Council (BMRC) and by a Wellcome Trust Programme Grant [082962 to P.W.I. and F.v.E.]. Deposited in PMC for release after 6 months.

Competing interests statement
The authors declare no competing financial interests.

Supplementary material
Supplementary material available online at
http://dev.biologists.org/lookup/suppl/doi:10.1242/dev.070862/-/DC1

References

Bai, C. B. and Joyner, A. L. (2001). *Gli1* can rescue the in vivo function of *Gli2*. *Development* **128**, 5161-5172.
Bangs, F., Antonio, N., Thongnuek, P., Welten, M., Davey, M. G., Briscoe, J., Tickle, C. (2011). Generation of a transgenic mouse with functional inactivation of *talpid3*, a gene first identified in chickens. *Development* **138**, 3261-3272.
Barth, K. A. and Wilson, S. W. (1995). Expression of zebrafish *nk2.2* is influenced by *sonic hedgehog/vertebrate hedgehog-1* and demarcates a zone of neuronal differentiation in the embryonic forebrain. *Development* **121**, 1755-1768.
Chen, J. N., van Bebber, F., Goldstein, A. M., Serluca, F. C., Jackson, D., Childs, S., Serbedzija, G., Warren, K. S., Mably, J. D., Lindahl, P. et al. (2001). Genetic steps to organ laterality in zebrafish. *Comp. Funct. Genomics* **2**, 60-68.
Ciruna, B., Weidinger, G., Knaut, H., Thisse, B., Thisse, C., Raz, E. and Schier, A. F. (2002). Production of maternal-zygotic mutant zebrafish by germ-line replacement. *Proc. Natl. Acad. Sci. USA* **99**, 14919-14924.
Concordet, J. P., Lewis, K. E., Moore, J. W., Goodrich, L. V., Johnson, R. L., Scott, M. P. and Ingham, P. W. (1996). Spatial regulation of a zebrafish *patched* homologue reflects the roles of sonic hedgehog and protein kinase A in neural tube and somite patterning. *Development* **122**, 2835-2846.
Davey, M. G., Paton, I. R., Yin, Y., Schmidt, M., Bangs, F. K., Morrice, D. R., Smith, T. G., Buxton, P., Stamataki, D., Tanaka, M. et al. (2006). The chicken *talpid3* gene encodes a novel protein essential for Hedgehog signaling. *Genes Dev.* **20**, 1365-1377.
Doyon, Y., McCammon, J. M., Miller, J. C., Faraji, F., Ngo, C., Katibah, G. E., Amora, R., Hocking, T. D., Zhang, L., Rebar, E. J. et al. (2008). Heritable targeted gene disruption in zebrafish using designed zinc-finger nucleases. *Nat. Biotechnol.* **26**, 702-708.
Drummond, I. A., Majumdar, A., Hentschel, H., Elger, M., Solnica-Krezel, L., Schier, A. F., Neuhauss, S. C., Stemple, D. L., Zwartkruis, F., Rangini, Z. et al. (1998). Early development of the zebrafish pronephros and analysis of mutations affecting pronephric function. *Development* **125**, 4655-4667.
Ede, D. A., Bellairs, R. and Bancroft, M. (1974). A scanning electron microscope study of the early limb-bud in normal and *talpid3* mutant chick embryos. *J. Embryol. Exp. Morphol.* **31**, 761-785.
Ede, D. A. and Kelly, W. A. (1964). Developmental abnormalities in the trunk and limbs of the *Talpid3* mutant of the fowl. *J. Embryol. Exp. Morphol.* **12**, 339-356.
Eggenschwiler, J. T. and Anderson, K. V. (2007). Cilia and developmental signaling. *Annu. Rev. Cell Dev. Biol.* **23**, 345-373.
Eisen, J. S. and Smith, J. C. (2008). Controlling morpholino experiments: don't stop making antisense. *Development* **135**, 1735-1743.
Elworthy, S., Hargrave, M., Knight, R., Mebus, K. and Ingham, P. W. (2008). Expression of multiple slow myosin heavy chain genes reveals a diversity of zebrafish slow twitch muscle fibres with differing requirements for Hedgehog and Prdm1 activity. *Development* **135**, 2115-2126.
Foley, J. E., Yeh, J. R., Maeder, M. L., Reyon, D., Sander, J. D., Peterson, R. T. and Joung, J. K. (2009). Rapid mutation of endogenous zebrafish genes using zinc finger nucleases made by Oligomerized Pool ENgineering (OPEN). *PLoS One* **4**, e4348.
Glazer, A. M., Wilkinson, A. W., Backer, C. B., Lapan, S. W., Gutzman, J. H., Cheeseman, I. M. and Reddien, P. W. (2010). The Zn finger protein Iguana impacts Hedgehog signaling by promoting ciliogenesis. *Dev. Biol.* **337**, 148-156.
Haffter, P. and Nüsslein-Volhard, C. (1996). Large scale genetics in a small vertebrate, the zebrafish. *Int. J. Dev. Biol.* **40**, 221-227.
Head, M. W., Triplett, E. L., Ede, D. A. and Clayton, R. M. (1992). Localization of delta-crystallin RNA during lens morphogenesis and differentiation in the normal and *talpid3* chick embryo. *Int. J. Dev. Biol.* **36**, 363-372.
Hinchliffe, J. R. and Thorogood, P. V. (1974). Genetic inhibition of mesenchymal cell death and the development of form and skeletal pattern in the limbs of *talpid3* (*ta3*) mutant chick embryos. *J. Embryol. Exp. Morphol.* **31**, 747-760.
Hirokawa, N., Tanaka, Y., Okada, Y. and Takeda, S. (2006). Nodal flow and the generation of left-right asymmetry. *Cell* **125**, 33-45.
Huang, P. and Schier, A. F. (2009). Dampened Hedgehog signaling but normal Wnt signaling in zebrafish without cilia. *Development* **136**, 3089-3098.
Ingham, P. W., Nakano, Y. and Seger, C. (2011). Mechanisms and functions of Hedgehog signalling across the metazoa. *Nat. Rev. Genet.* **12**, 393-406.
Ingham, P. W. and Placzek, M. (2006). Orchestrating ontogenesis: variations on a theme by Sonic Hedgehog. *Nat. Rev. Genet.* **7**, 841-850.
Karlstrom, R. O., Talbot, W. S. and Schier, A. F. (1999). Comparative synteny cloning of zebrafish *you-too*: mutations in the Hedgehog target *gli2* affect ventral forebrain patterning. *Genes Dev.* **13**, 388-393.
Karlstrom, R. O., Tyurina, O. V., Kawakami, A., Nishioka, N., Talbot, W. S., Sasaki, H. and Schier, A. F. (2003). Genetic analysis of zebrafish *gli1* and *gli2* reveals divergent requirements for *gli* genes in vertebrate development. *Development* **130**, 1549-1564.
Ke, Z., Kondrichin, I., Gong, Z. and Korzh, V. (2008). Combined activity of the two *Gli2* genes of zebrafish play a major role in Hedgehog signaling during zebrafish neurodevelopment. *Mol. Cell. Neurosci.* **37**, 388-401.
Kim, H. R., Richardson, J., van Eeden, F. and Ingham, P. W. (2010). Gli2a protein localization reveals a role for Iguana/DZIP1 in primary ciliogenesis and a dependence of Hedgehog signal transduction on primary cilia in the zebrafish. *BMC Biol.* **8**, 65.
Koprunner, M., Thisse, C., Thisse, B. and Raz, E. (2001). A zebrafish *nanos*-related gene is essential for the development of primordial germ cells. *Genes Dev.* **15**, 2877-2885.
Koudijs, M. J., den Broeder, M. J., Groot, E. and van Eeden, F. J. (2008). Genetic analysis of the two zebrafish *patched* homologues identifies novel roles for the hedgehog signaling pathway. *BMC Dev. Biol.* **8**, 15.
Lawson, N. D. and Weinstein, B. M. (2002). In vivo imaging of embryonic vascular development using transgenic zebrafish. *Dev. Biol.* **248**, 307-318.

Lee, K. K. and Ede, D. A. (1989). The capacity of normal and *talpid3* mutant fowl myogenic cells to migrate in quail limb buds. *Anat. Embryol.* **179**, 395-402.
Levin, M., Johnson, R. L., Stern, C. D., Kuehn, M. and Tabin, C. (1995). A molecular pathway determining left-right asymmetry in chick embryogenesis. *Cell* **82**, 803-814.
Lewis, K. E., Drossopoulou, G., Paton, I. R., Morrice, D. R., Robertson, K. E., Burt, D. W., Ingham, P. W. and Tickle, C. (1999). Expression of *ptc* and *gli* genes in *talpid3* suggests bifurcation in Shh pathway. *Development* **126**, 2397-2407.
Litingtung, Y., Dahn, R. D., Li, Y., Fallon, J. F. and Chiang, C. (2002). Shh and Gli3 are dispensable for limb skeleton formation but regulate digit number and identity. *Nature* **418**, 979-983.
Lo, J., Lee, S., Xu, M., Liu, F., Ruan, H., Eun, A., He, Y., Ma, W., Wang, W., Wen, Z. et al. (2003). 15000 unique zebrafish EST clusters and their future use in microarray for profiling gene expression patterns during embryogenesis. *Genome Res.* **13**, 455-466.
Lunt, S. C., Haynes, T. and Perkins, B. D. (2009). Zebrafish *ift57*, *ift88*, and *ift172* intraflagellar transport mutants disrupt cilia but do not affect hedgehog signaling. *Dev. Dyn.* **238**, 1744-1759.
Maeder, M. L., Thibodeau-Beganny, S., Osiak, A., Wright, D. A., Anthony, R. M., Eichtinger, M., Jiang, T., Foley, J. E., Winfrey, R. J., Townsend, J. A. et al. (2008). Rapid 'open-source' engineering of customized zinc-finger nucleases for highly efficient gene modification. *Mol. Cell* **31**, 294-301.
Maurya, A. K., Tan, H., Souren, M., Wang, X., Wittbrodt, J. and Ingham, P. W. (2011). Integration of Hedgehog and BMP signalling by the *engrailed2a* gene in the zebrafish myotome. *Development* **138**, 755-765.
Meng, X., Noyes, M. B., Zhu, L. J., Lawson, N. D. and Wolfe, S. A. (2008). Targeted gene inactivation in zebrafish using engineered zinc-finger nucleases. *Nat. Biotechnol.* **26**, 695-701.
Motoyama, J., Milenkovic, L., Iwama, M., Shikata, Y., Scott, M. P. and Hui, C. C. (2003). Differential requirement for Gli2 and Gli3 in ventral neural cell fate specification. *Dev. Biol.* **259**, 150-161.
Noyes, M. B., Meng, X., Wakabayashi, A., Sinha, S., Brodsky, M. H. and Wolfe, S. A. (2008). A systematic characterization of factors that regulate *Drosophila* segmentation via a bacterial one-hybrid system. *Nucleic Acids Res.* **36**, 2547-2560.
Oxtoby, E. and Jowett, T. (1993). Cloning of the zebrafish *krox-20* gene (*krx-20*) and its expression during hindbrain development. *Nucleic Acids Res.* **21**, 1087-1095.
Pan, Y., Bai, C. B., Joyner, A. L. and Wang, B. (2006). Sonic hedgehog signaling regulates Gli2 transcriptional activity by suppressing its processing and degradation. *Mol. Cell. Biol.* **26**, 3365-3377.
Pan, Y. and Wang, B. (2007). A novel protein-processing domain in Gli2 and Gli3 differentially blocks complete protein degradation by the proteasome. *J. Biol. Chem.* **282**, 10846-10852.
Pathak, N., Obara, T., Mangos, S., Liu, Y. and Drummond, I. A. (2007). The zebrafish *fleer* gene encodes an essential regulator of cilia tubulin polyglutamylation. *Mol. Biol. Cell* **18**, 4353-4364.
Ramirez, C. L., Foley, J. E., Wright, D. A., Muller-Lerch, F., Rahman, S. H., Cornu, T. I., Winfrey, R. J., Sander, J. D., Fu, F., Townsend, J. A. et al. (2008). Unexpected failure rates for modular assembly of engineered zinc fingers. *Nat. Methods* **5**, 374-375.
Roy, S., Qiao, T., Wolff, C. and Ingham, P. W. (2001). Hedgehog signaling pathway is essential for pancreas specification in the zebrafish embryo. *Curr. Biol.* **11**, 1358-1363.
Schilling, T. F., Concordet, J. P. and Ingham, P. W. (1999). Regulation of left-right asymmetries in the zebrafish by Shh and BMP4. *Dev. Biol.* **210**, 277-287.
Sekimizu, K., Nishioka, N., Sasaki, H., Takeda, H., Karlstrom, R. O. and Kawakami, A. (2004). The zebrafish *iguana* locus encodes Dzip1, a novel zinc-finger protein required for proper regulation of Hedgehog signaling. *Development* **131**, 2521-2532.
Sun, Z., Amsterdam, A., Pazour, G. J., Cole, D. G., Miller, M. S. and Hopkins, N. (2004). A genetic screen in zebrafish identifies cilia genes as a principal cause of cystic kidney. *Development* **131**, 4085-4093.
Tay, S. Y., Ingham, P. W. and Roy, S. (2005). A homologue of the *Drosophila* kinesin-like protein Costal2 regulates Hedgehog signal transduction in the vertebrate embryo. *Development* **132**, 625-634.
Tay, S. Y., Yu, X., Wong, K. N., Panse, P., Ng, C. P. and Roy, S. (2010). The iguana/DZIP1 protein is a novel component of the ciliogenic pathway essential for axonemal biogenesis. *Dev. Dyn.* **239**, 527-534.
Turner, D. L. and Weintraub, H. (1994). Expression of achaete-scute homolog 3 in *Xenopus* embryos converts ectodermal cells to a neural fate. *Genes Dev.* **8**, 1434-1447.
Tyurina, O. V., Guner, B., Popova, E., Feng, J., Schier, A. F., Kohtz, J. D. and Karlstrom, R. O. (2005). Zebrafish Gli3 functions as both an activator and a repressor in Hedgehog signaling. *Dev. Biol.* **277**, 537-556.
Wang, B., Fallon, J. F. and Beachy, P. A. (2000). Hedgehog-regulated processing of Gli3 produces an anterior/posterior repressor gradient in the developing vertebrate limb. *Cell* **100**, 423-434.
Weidinger, G., Stebler, J., Slanchev, K., Dumstrei, K., Wise, C., Lovell-Badge, R., Thisse, C., Thisse, B. and Raz, E. (2003). dead end, a novel vertebrate germ plasm component, is required for zebrafish primordial germ cell migration and survival. *Curr. Biol.* **13**, 1429-1434.
Wolff, C., Roy, S. and Ingham, P. W. (2003). Multiple muscle cell identities induced by distinct levels and timing of hedgehog activity in the zebrafish embryo. *Curr. Biol.* **13**, 1169-1181.
Wolff, C., Roy, S., Lewis, K. E., Schauerte, H., Joerg-Rauch, G., Kirn, A., Weiler, C., Geisler, R., Haffter, P. and Ingham, P. W. (2004). *iguana* encodes a novel zinc-finger protein with coiled-coil domains essential for Hedgehog signal transduction in the zebrafish embryo. *Genes Dev.* **18**, 1565-1576.
Yin, Y., Bangs, F., Paton, I. R., Prescott, A., James, J., Davey, M. G., Whitley, P., Genikhovich, G., Technau, U., Burt, D. W. et al. (2009). The *Talpid3* gene (KIAA0586) encodes a centrosomal protein that is essential for primary cilia formation. *Development* **136**, 655-664.